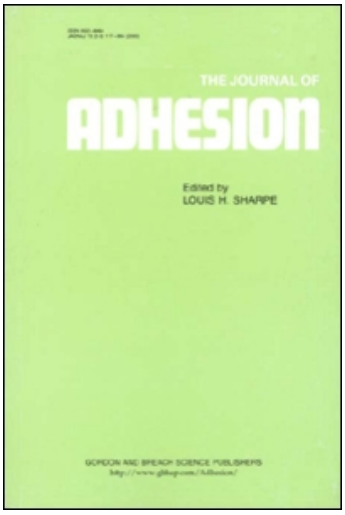

The Journal of Adhesion
Publication details, including instructions for authors and subscription information:
http://www.informaworld.com/smpp/title~content=t713453635

Adhesion Tensile Testing of Environmentally Exposed Ti-6Al-4V Adherends

H. M. Clearfield[a]; D. K. Shaffer[a]; J. S. Ahearn[a]; J. D. Venables[a]
[a] Martin Marietta Laboratories, Baltimore, MD, U.S.A.

To cite this Article Clearfield, H. M. , Shaffer, D. K. , Ahearn, J. S. and Venables, J. D.(1987) 'Adhesion Tensile Testing of Environmentally Exposed Ti-6Al-4V Adherends', The Journal of Adhesion, 23: 2, 83 — 97
To link to this Article: DOI: 10.1080/00218468708075398
URL: http://dx.doi.org/10.1080/00218468708075398

J. Adhesion, 1987, Vol. 23, pp. 83–97
Photocopying permitted by license only

Printed in the United Kingdom

Adhesion Tensile Testing of Environmentally Exposed Ti-6Al-4V Adherends†

H. M. CLEARFIELD, D. K. SHAFFER, J. S. AHEARN, and J. D. VENABLES

Martin Marietta Laboratories, 1450 S. Rolling Road, Baltimore, MD 21227, U.S.A.

(Received September 4, 1986)

The structural and bonding properties of Ti-6Al-4V adherends, prepared by chromic acid anodization (CAA), were studied as a function of exposure in high-temperature environments such as vacuum, air, boiling and pressurized water, and steam. Subsequent to the environmental exposure, bonds were produced and the adhesive tensile strengths measured. Long-term exposure to high temperature, dry environments did not cause structural changes to the adherend oxide but did result in poor bond strength. The failure mode in these cases was within the oxide, which was apparently weakened by the exposure. The water- and steam-exposed oxides underwent a transition from amorphous to crystalline TiO_2 (with an accompanying change in oxide morphology); however, bond strength was maintained for moderate exposures at $T \leq 250°C$. For exposure at $T = 300°C$, the bond strength was degraded severely. The latter result can be explained by a lack of porosity in the transformed oxide. SEM and XPS measurements were made on debonded surfaces to determine the loci of failure.

KEY WORDS Titanium adhesive bonding; oxide morphology; environmental exposures; adherend surface analysis; Ti-6Al-4V; oxide stability.

I INTRODUCTION

Adhesively bonded materials that are stable at high temperatures are becoming increasingly important for the performance of

† Presented at the Tenth Annual Meeting of The Adhesion Society, Inc., Williamsburg, Virginia, U.S.A., February 22–27, 1987.

advanced military and aerospace systems. The proposed operating temperature range, from 100–400°C, presents special problems for all components of the bonded system, *i.e.*, adherend, primer and adhesive must all be stable in severe environments. Several classes of metal adherends are used (or have been proposed) for such systems, including titanium alloys, nickel-based superalloys, and high-temperature steels. One, Ti-6Al-4V, is a particularly good baseline material for the adherend because its mechanical properties are retained at high temperatures.

In previous studies of both Ti[1] and Al[2,3] adhesive bonding systems, it was shown that initial bond strength was enhanced by physical interlocking between the adherend oxide and the adhesive; porous oxides maximized this interlocking and hence provided the best overall bond strength. Additionally, in Al adherends, humidity-induced changes in the oxide led to bond degradation. The primary cause of failure in that case was the transformation of the original oxide to a hydroxide that is loosely bound to the Al substrate.[3] Certain organic inhibitors were later used to slow down such a transformation, thereby increasing bond durability.[4]

The oxide of Ti, typically formed by anodization in a chromic acid solution (CAA), is much more stable than that of Al and hence the bonds exhibit markedly better durability. However, the unbonded Ti oxide was found to undergo a transition from amorphous TiO_2 to crystalline TiO_2 (anatase) when immersed in water at 85°C for as little as 20 hours.[5] The transformation was accompanied by a change in morphology—from a porous, honeycomb structure to a more needle-like structure. Although some porosity was retained after this transformation, it was later shown that exposure to humid environments for longer times or at higher temperatures results eventually in a rather smooth, nodular-like oxide that lacks porosity.[6]

The observation that a CAA oxide that was transformed at lower temperatures retained porosity suggests that such an oxide might couple mechanically to an adhesive. It would be desirable to use such a transformed oxide in a bondline, if the oxide-base metal interfacial strength were maintained, because the crystalline Ti oxide phases are more stable thermodynamically than the amorphous phase.[7] Although anatase is not the most stable form of TiO_2,[7] none of the other crystalline TiO_2 phases has been observed

in earlier Ti adherend studies (the anatase to rutile transformation occurs at ~650°C at atmospheric pressure—the earlier studies were conducted at lower temperatures).[5,6] Thus, by bonding to a crystalline adherend oxide, *i.e.*, anatase, large-scale morphology changes that normally occur during accelerated testing could presumably be avoided, thereby increasing bond durability.

In this study, we have investigated the strength of bonds formed on Ti-6Al-4V adherends after they were subjected to high-temperature environments such as vacuum, air, boiling water, pressurized water and steam. The CAA oxide was chosen as the baseline adherend because it provides excellent bond durability for Ti adhesive bonds.[1] Coupons were anodized, exposed, bonded to an Al stud (see below), and tested with an instrument that applies a tensile force normal to the adherend surface. The test was designed to determine the adhesion of the (transformed) oxide to the underlying substrate. Adherends were characterized before and after tensile testing by high-resolution scanning electron microscopy (SEM) and X-ray photoelectron spectroscopy (XPS). These measurements allowed the identification of the loci of failure in the adhesion tensile tests. The failure mechanisms were then correlated with the respective oxide morphologies.

II EXPERIMENTAL

A Sample preparation

Coupons of Ti-6Al-4V were anodized in a solution containing 5% chromic acid (CAA). Details of the procedure are given elsewhere.[6,8] Transmission electron micrographs show that the resultant oxide is ~120 nm thick and amorphous.[6]

Coupons subjected to heat alone were placed in a vacuum furnace for periods of 72 and 160 hr at 400°C, and at a pressure of 3×10^{-4} Pa. Although there was no residual gas analyzer on the furnace, we estimate the partial pressure of oxygen to be less than 5×10^{-5} Pa.[9] Any residual water vapor was pumped away during warmup. Additionally, some coupons were exposed to air in an ordinary laboratory furnace at 330°C. Exposure times varied from 160–1200 hr. The relative humidity in the furnace was not determined.

The boiling water exposures were conducted by immersion of the coupons in water maintained at 95–100°C. For higher temperature water exposures, a high-pressure autoclave was used. In this case, a sufficient volume of water was used at each temperature to maintain an equilibrium between liquid and vapor at the saturation vapor pressure. Some coupons were immersed in the liquid; others were exposed only to the vapor. Exposures ranged from 3–120 hr at temperatures of 150, 200, 250 and 300°C.

B Adhesion testing

A pneumatic adhesion tensile testing instrument (SEMicro, Rockville, MD) was used for the adhesion tests. A schematic drawing of the testing geometry is shown in Figure 1. A 1.25-cm-diameter Al stud (that had been etched previously in FPL solution) was bonded to the pre-exposed adherend with an epoxy resin (3M 1838). The bonding area was defined with a Teflon ring. The adhesive was cured under a pressure of 0.4 MPa for 72 hr at room temperature; the thickness of the bondline was not determined. Prior to testing, the Teflon ring was replaced by a stainless steel ring and the bonded system was mounted in a jig that prevents the adherend from flexing. The stud was screwed into a pneumatic piston which applies the tensile force (increasing at ~4 MPa/min) normal to the adherend surface. The force required to remove the stud thus provides a relative indication of the bond strength of the oxide.

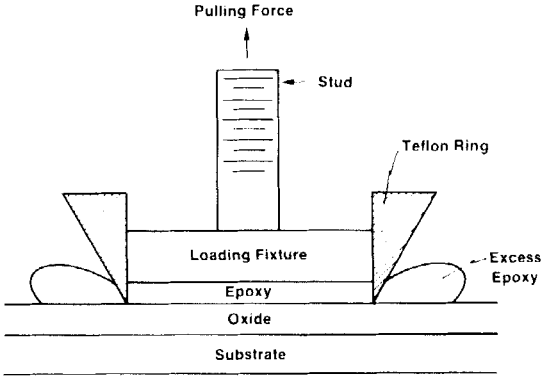

FIGURE 1 Schematic diagram of adhesion tensile testing geometry.

C Analysis

A JEOL JEM 100-CX STEM, used in the SEM mode, provided the resolution needed to examine the morphology of the CAA oxide and the bond-failure surfaces. Samples were cut to 1 cm × 2 mm and coated with ~5 nm of Pt to eliminate charge buildup on the oxide. The stereo micrographs shown in this study were obtained at ±7 deg tilt.

XPS was used to determine the surface composition of the oxides and the debonded surfaces. The spectrometer, an SSL SSX-100, was equipped with a differentially-pumped ion sputter gun. For compositional analysis, the analyzed area was 600 μm in diameter, which was large enough to represent the average over the entire coupon surface. For depth profiles, a 300-μm-diameter area at the center of a 3 mm × 3 mm crater was used.

III RESULTS AND DISCUSSION

A Morphology of exposed adherends

A stereo micrograph of a typical, as-anodized CAA oxide is shown in Figure 2. It is characterized by a multilevel, porous structure with cell dimensions on the order of 40 nm. At lower magnifications (Figure 2a), it is evident that the porous structure covers the entire surface. The multilevel morphology is due to differential etching of the two-phase alloy.

Samples that were exposed to vacuum at 400°C for as long as 160 hr showed no change in morphology when examined by SEM, *i.e.*, the porous, honeycomb morphology was retained. However, in a micrograph of a sample exposed to air at 330°C for 1200 hr, Figure 3, the honeycomb structure is still evident but the cell walls have thickened slightly. Additionally, some peeling of the oxide seems to have occurred at the grain boundaries.

CAA oxides immersed in boiling water developed crystallites, consistent with earlier results.[1,5] After as little as 3 hr immersion, the honeycomb cell walls begin to thicken. By 24 hr, crystallites can be observed and the cells have nearly closed up. By 72 hr, the adherend surface is covered with crystallites and the honeycomb structure has disappeared, as seen in Figure 4. Some fusion of the

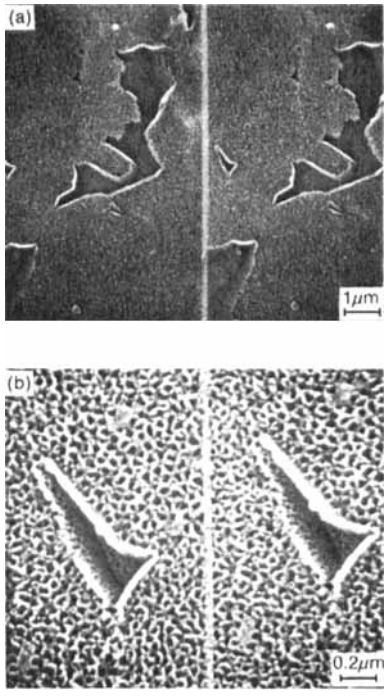

FIGURE 2 Scanning electron micrographs at a) low and b) high magnification, showing the oxide surface resulting from the anodization of Ti-6Al-4V adherends in a solution containing 5% chromic acid.

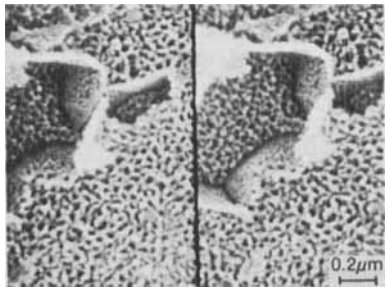

FIGURE 3 CAA oxide after heating in air at 330°C for 1200 hours. Some thickening of the cell walls has occurred.

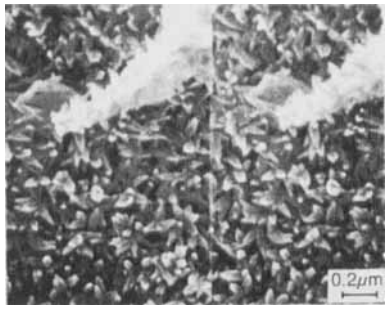

FIGURE 4 CAA oxide after immersion in water at 100°C for 72 hours.

crystallites has also occurred. A dissolution/precipitation mechanism for this change in morphology has been proposed in Reference 6.

As already mentioned, some CAA oxides exposed to water in the autoclave were immersed in the liquid, while others that hung above the liquid were exposed only to the vapor. The evolution of the oxide is different for the two exposures, as can be seen in the sequence of Figures 5a–c. Those immersed in the liquid at 300°C were completely covered by needle-like crystallites after as little as 3 hr (Figure 5a). By 24 hr (Figure 5b), the crystallites began to fuse and the surface appears somewhat flatter. Finally, at 120 hr (Figure 5c), the crystallites became nodular in shape, leaving an oxide that was relatively smooth (compared to the as-anodized oxide). For vapor-exposed oxides, no needle-like crystallites were observed. Rather, the honeycomb structure evolved into a more nodular-like oxide (Figure 5a). Selected area diffraction (SAD) patterns generated in the TEM show these nodules to be anatase TiO_2. With continued exposure, the nodules began to fuse (Figure 5b) until, by 120 hr, the oxide surface was again relatively smooth, *i.e.*, lacking porisity (Figure 5c). The diameter of the vapor-exposed nodules was approximately one-half that of the corresponding liquid-exposed nodules.

B Adhesion tensile tests

1 *As-anodized adherends* The tensile test used in this study measured the relative adhesive strength of the oxide-base metal

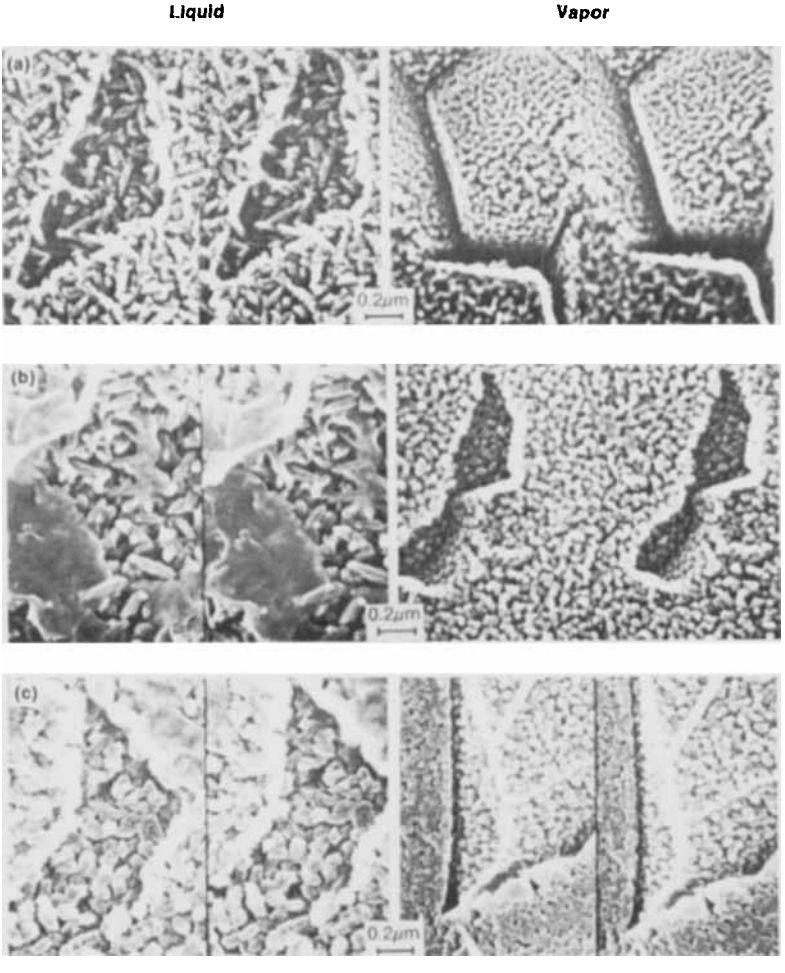

FIGURE 5 CAA oxide after exposure to water in liquid and vapor phases in an autoclave at 300°C: a) 3, b) 24 and c) 120 hours.

interface. The results are presented in Table I. The greatest bond strength was obtained with the as-anodized CAA oxide. Visual examination of the debonded surfaces showed both to have the same appearance—rough and of the same color as the adhesive—suggesting that the failure mode was cohesive. To confirm this, we examined the surfaces by SEM and XPS. Scanning electron

TABLE I
Adhesion tensile test results

Ti-6Al-4V (CAA 5%) Exposure	Pull strength (MPa)
As-anodized	9.2 ± 0.5(cohesive)*
Vacuum ($T = 400°C$)	0–0.7(oxide)
Air 330°C, 160 hr	3.5(mixed)
Air 330°C, 1200 hr	0–0.7(oxide)
Boiling/pressurized water, steam ($T \leq 250°C$)	6.2–8.3(mixed)
Pressurized water, steam ($T = 300°C$)	0–0.7(adhesive)

* Failure mode is indicated in parentheses.

micrographs showed an adhesive-like morphology on both sides with large (20-μm-diameter; Figure 6) filler particles consisting primarily of Al and Si. The XPS spectra obtained from the metal and the ahdesive sides of the failure are nearly identical to each other, as shown in Figure 7, and to spectra obtained from the cured adhesive alone. The C and O concentrations are indicative of the adhesive component, and the Al and Si from the filler particles are evident. We conclude that 9.2 MPa (Table I) represents the cohesive strength of the adhesive in this testing geometry. This value is significantly less that that quoted by the manufacturer, and can be attributed to some flexing of the adherend. Thicker adherends used in the same geometry yield cohesive strengths that approach the manufacturers' value.[10]

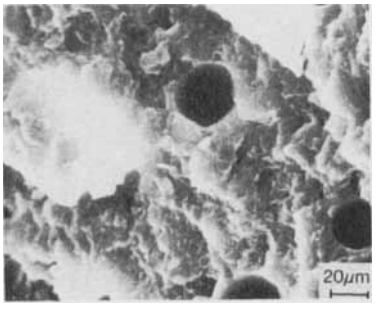

FIGURE 6 Typical scanning electron micrograph of both debonded surfaces of an as-anodized Ti-6Al-4V adherend. The morphology is indicative of adhesive on both sides of the failure.

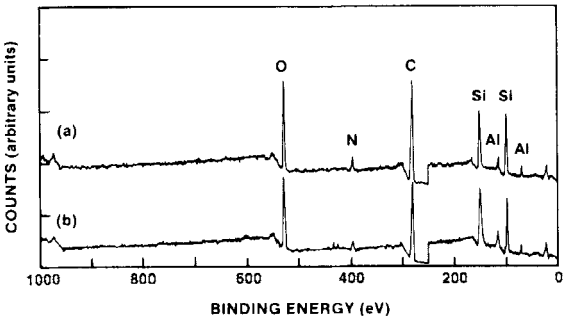

FIGURE 7 X-ray photoelectron spectra of a) metal and b) stud sides of an as-anodized Ti-6Al-4V adherend after tensile testing. The spectra are typical of adhesive.

2 *Vacuum- and air-exposed adherends* Most of the high-temperature vacuum- and air-exposed specimens failed prior to testing as the Teflon ring was being removed. Those that were tested failed at pressures less than 0.7 MPa. The debonded surfaces appeared metallic on both the stud and the metal sides, indicating failure entirely within the oxide layer or at the oxide–metal interface. The precise location was determined by SEM and XPS depth profiles. As seen in Figure 8 (the stud side), the original CAA oxide cell walls are evident and have lifted away from the base metal. The micrograph from the metal side shows a complementary

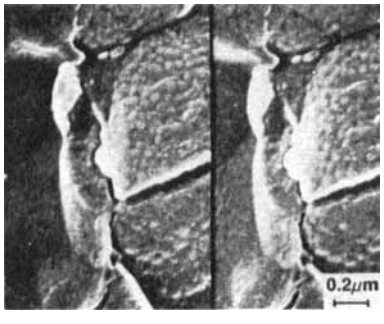

FIGURE 8 Debonded surface from the stud side of a Ti-6Al-4V adherend exposed to air for 1200 hr at 330°C, after tensile testing. A replica of a honeycomb structure is evident, indicating that the oxide has been lifted from the adherend.

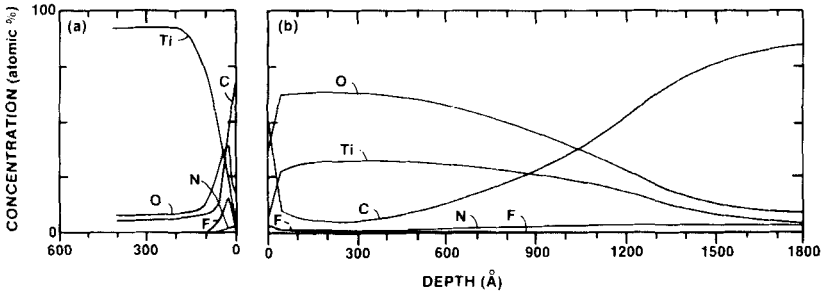

FIGURE 9 XPS depth profiles of the debonded surface from the a) metal and b) stud side of a Ti-6Al-4V adherend exposed to air for 1200 hr at 330°C, after tensile testing.

image. XPS survey spectra of both surfaces were identical; however, depth profiles show different oxide layer thicknesses. On the metal side, Figure 9a, the oxide-metal interface is abrupt and appears at a depth less than 10 nm as judged by the rapid increase in the Ti signal with depth (the greatest oxide layer thickness on the metal side of any of these samples was ~30 nm). In Figure 9b, the stud side, the oxide-adhesive interface is not well defined due to penetration of the adhesive into the honeycomb structure. One feature common to both depth profiles is the accumulaton of F at both debonded surfaces. Previously, we found an accumulation of F near the oxide–metal interface in as-anodized and air-exposed oxides.[6] Cross-sectional TEM revealed that the oxide consisted of a 20- to 30-nm-thick barrier layer under the honeycomb structure (~100 nm thick). Thus, the depth profile in Figure 9b can be described in terms of three distinct regions: at depths less than 30 nm, the profile is dominated by the steady level of the Ti and O signals, and C is at its background level. This corresponds to the barrier layer. Between 30 and 140 nm, the steady rise in C concentration indicates that the adhesive penetrated the oxide. At depths greater than 140 nm, the C signal is dominant, indicative of the adhesive layer. We conclude from the micrographs and the depth profiles that the debonding occured within the barrier layer at or very near the oxide-metal interface.

The failure at low stress levels of vacuum- and air-exposed oxides was surprising in view of the retention of the honeycomb structure

after exposure, especially since earlier studies indicated that porous oxides were important for bond durability. In an effort to understand this, we subsequently cycled some of the pre-exposed adherends from room temperature to 400°C several times under vacuum. The vacuum- and air-exposed adherends developed large cracks eventually whereas water-exposed adherends did not. The cracks may have developed due to stress between the untransformed oxide and the base metal (at the barrier layer) during cycling. This is reasonable in that there is a 5% difference between the thermal expansion coefficients of Ti and TiO_2.[11] Earlier cross-sectional TEM measurements of the water-exposed oxides showed that the barrier layer had disappeared with the transformation to the anatase phase.[6] Therefore, the water-exposed oxides may not have experienced the same stresses as the vacuum-exposed oxides during thermal cycling and did not develop cracks.

An alternate explanation for the loss of bond strength is a change in the microstructure of the Ti-6Al-4V during heating. Typically, Ti-6Al-4V is rolled into sheets at $T \simeq 900°C$ and subsequently cooled rapidly. This results in a non-equilibrium microstructure that contains a significant volume fraction of metastable beta phase (*i.e.*, V-stabilized). Annealing at $T \geqslant 300°C$ can cause the metastable beta to transform to the alpha phase, thereby disrupting the oxide-metal interface. Optical micrographs obtained from as-anodized and air-exposed adherends support this hypothesis.[12]

3 *Boiling, pressurized water- and steam-exposed adherends* CAA oxides exposed to both liquid and vapor environments at tempertures below 250°C retained almost all of their bond strength, as seen in Table I. Although these debonded surfaces were not examined by XPS, the appearance of adhesive material on all of them suggests that the failure mode was predominantly cohesive in each case (although small areas of adhesive failure could be delineated). It should be noted that the tensile strength values listed for water-exposed adherends in Table I represent the averages of many samples. Some of these exhibited tensile strengths comparable to those obtained for the as-anodized adherends.

Adherends exposed to humid environments at 300°C for 24 hr or more failed at low stress levels. In these cases, the two debonded surfaces appeared different, suggesting an adhesive failure mode.

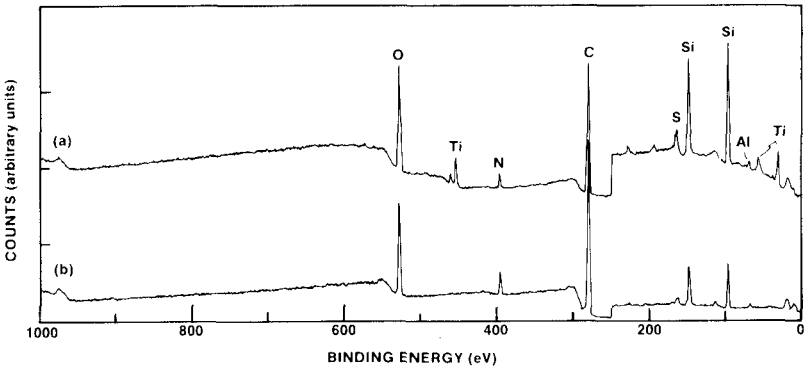

FIGURE 10 X-ray photoelectron spectra of a) metal and b) stud side of a Ti-6Al-4V adherend exposed to steam in a high-pressure autoclave for 120 hours at 300°C, after tensile testing.

This was confirmed by XPS measurements. In Figure 10a, the spectrum obtained from the metal side contains a significant concentration of Ti although the C and Si concentrations are much greater than those observed for the as-anodized surface. Two explanations for the enhanced C and Si are plausible: the increased concentrations may be due either to a very thin adhesive layer (2–4 nm thick) left after the tensile test or to contamination during transfer to the XPS vacuum system. The spectrum of the stud side, Figure 10b, shows no Ti but is typical of the adhesive alone. Scanning electron micrographs show adhesive on the stud side and the nodular oxide on the metal side of the failure.

Selected area diffraction patterns obtained from water- and vapor-exposed adherends show that the oxide is crystalline TiO_2. The tensile test results indicate, at least for temperatures below 250°C, that the integrity of the oxide-metal interface is retained despite the amorphous-to-crystalline (structural) transformation—the transformed oxide itself can be bonded with nearly the same strength as the as-anodized oxide. This result is in contrast with those obtained for Al adherends that were exposed while bonded, in which chemical changes result in weak bonding to the base metal.[3] It is apparent from the SEM micrographs that porosity exists in water-exposed surfaces even after the transformation and,

therefore, the adhesive can penetrate and interlock mechanically with the oxide.

The lack of porosity can explain the reduced bond strength in adherends exposed to humid environments for the longest times and/or at the highest temperatures. In these instances, the adhesive cannot penetrate the oxide and, therefore, no mechanical coupling can occur. The adhesive merely pulls away from the oxide under very little tensile force.

IV SUMMARY

Tensile testing of Ti-6Al-4V adherends that were exposed to a variety of high-temperature environments prior to testing indicate that the mode of failure depended on the nature of the environmental exposure. The as-anodized adherends all failed cohesively (within the adhesive itself). Although the original CAA morphology was retained after high-temperature exposures in vacuum and air, adherends subjected to these environments at temperatures greater than (or equal to) 330°C degraded severely and failed within the oxide. Oxides subjected to moderate, humid environments retained almost all of their initial bond strength although long-term or high-temperature exposures resulted in adhesive failures.

The tensile tests were not designed to simulate phenomena that would occur in a bondline. Such simulations are usually done using, for instance, wedge-crack propagation tests. Structural transformations of the magnitude we have observed would likely result in drastic bond failures if they occurred in a bondline. Rather, the tensile test results suggest that a pre-transformed, crystalline oxide might be used as a suitable alternative to an amorphous oxide in a bondline because the crystalline oxide is more stable thermodynamically. It has been shown that annealing alone can transform amorphous TiO_2 films to crystalline ones[13] so it may also be possible to transform the oxide in a non-humid environment. We are presently exploring these possibilities.

Acknowledgements

We acknowledge useful discussions with D. McNamara, G. Davis and A. Desai. G. Cote acquired much of the XPS data. P. Martin assisted with the tensile tests. The

financial support of DARPA/ONR under contract number N00014-85-C-0804 is gratefully acknowledged.

References

1. B. M. Ditchek, *et al., Proc. 25th Natl. SAMPE Symp. Exhib.,* San Diego, CA, U.S.A., 1980 (SAMPE, Azusa, CA, 1980).
2. Reviews of some earlier Ti and Al adhesive bonding studies can be found in J. D. Venables, *J. Mater. Sci.* **19,** 2431 (1984) and A. J. Kinloch, *J. Mater. Sci.* **17,** 617 (1982).
3. J. D. Venables, *et al., Proc. 12th Natl. SAMPE Tech. Conf.,* Seattle WA, U.S.A., 1980 (SAMPE, Azusa, CA, 1980).
4. D. A. Hardwick, J. S. Ahearn, A. Desai and J. D. Venables, *J. Mater. Sci.* **21,** 179 (1986).
5. M. Natan and J. D. Venables, *J. Adhesion,* **15,** 125 (1983).
6. H. M. Clearfield, D. K. Shaffer and J. S. Ahearn, *Proc. 18th Natl. SAMPE Tech. Conf.,* Seattle, WA, U.S.A., 1986 (SAMPE, Azusa, CA, 1986), p. 921.
7. A. Matthews, *Am. Mineral.* **61,** 419 (1976).
8. Y. Moji and J. A. Marceau, U.S. Patent No. 3959091, assigned to the Boeing Company (1976).
9. P. A. Redhead, J. P. Hobson, and E. V. Kornelsen, *The Physical Basis of Ultrahigh Vacuum* (Chapman and Hall, London, 1968).
10. A. Desai, private communication.
11. A. Goldsmith, H. J. Hirschhorn, and T. E. Waterman, *Thermophysical Properties of Solid Materials,* Vol. II, WADC Tech. Rep. 58-476 (Wright Air Development Division, Dayton, OH, 1960).
12. H. M. Clearfield, C. P. Blankenship, D. K. Shaffer, and J. S. Ahearn, unpublished results.
13. L. S. Hsu, R. Rujkorakarn, J. R. Sites, and C. Y. She, *J. Appl. Phys.* **59,** 3475 (1986).